

Aharonov–Bohm Effect on Multiwall Carbon Nanotubes under Conditions Close to Strong Carrier Localization

Yu. I. Latyshev^a, A. P. Orlov^a, A. Yu. Latyshev^a, T. L. Wade^b,
M. Konczykowski^b, and P. Monceau^{c, d}

^a Kotel'nikov Institute of Radio Engineering and Electronics, Russian Academy of Sciences,
ul. Mokhovaya 17/78, Moscow, 125009 Russia
e-mail: yurilatyshev@yahoo.com

^b Laboratoire des Solides Irradiés, Ecole Polytechnique, 91128 Palaiseau Cedex, France

^c Institut Néel, 38042 Grenoble Cedex 9, France

^d Laboratoire National des Champs Magnétiques Intenses, 38042 Grenoble Cedex 9, France

Received September 30, 2009

The Aharonov–Bohm effect on multiwall carbon nanotubes has been studied under conditions of resistance with decreasing temperature as an inverse power function, which precede strong carrier localization. A periodic contribution with a period of 18 T corresponding to the magnetic flux quantum $\hbar c/e$ per nanotube cross section has been revealed in the longitudinal magnetoresistance. The result points to the possibility of the ballistic motion of the carriers over the sample perimeter under conditions close to their strong localization in the longitudinal direction.

PACS numbers: 72.15.Rn, 72.20.My, 73.68.Fg

DOI: 10.1134/S0021364009210048

Carbon nanotubes are one of the most interesting recently studied nanocarbon objects [1]. A nanotube can be represented as a graphene sheet folded along a certain crystallographic direction with a diameter of 1 to 30 nm. Single-wall nanotubes (SWNTs) and multiwall nanotubes (MWNTs) embedded into each other are known. The SWNT diameter is usually smaller than 2 nm, while the MWNT diameter is larger than 2–3 nm and reaches several tens of nanometers. The single-wall nanotubes are usually purer and their length is equal to the mean free path of the carriers, which is much larger than their diameter. The multiwall nanotubes are dirtier. The individual nanotubes of both modifications are of great interest in the investigation of quantum transport in the one-dimensional limit. Depending on their perfection degree, the ballistic mode [2, 3] and the weak localization mode [4] can be observed in them, while the transition to the strong localization mode is observed in the “dirtiest” nanotubes [5].

Owing to cylindrical topology, the quantum-interference phenomena of the carriers can be studied in the nanotubes in a magnetic field parallel to their axes. The flux quantization in the nanotube leads to magnetoresistance oscillations as the longitudinal magnetic field increases (the Aharonov–Bohm effect). In the ballistic mode, the period of oscillations in the flux is $\hbar c/e$ [6, 7]. In the weak localization mode, it is $\hbar c/2e$ [8] as has been observed earlier on the “dirty” metal cylindrical films [9] and theoretically predicted [10].

The factor 1/2 appears due to interference on direct and inverse trajectories. An interesting unstudied problem is the character of quantum interference under conditions close to the transition to the strong localization region. This region manifests itself on the nonmetal MWNTs and is characterized by the so-called zero anomaly—a dip of the differential conductivity $G = dI/dV$ at low bias voltages V [11]. In this case, the scaling relations are observed,

$$G(V \gg kT) \propto V^\alpha, \quad G(V \ll kT) \propto T^\alpha. \quad (1)$$

This behavior was explained in terms of the Luttinger liquid [12] and, recently, by the inelastic cotunneling processes on the high-resistance contacts in the MWNTs [13]. An alternative explanation employed the Coulomb blockade of the carriers in separate tunnel-bound MWNT segments [14].

This behavior was experimentally observed at low temperatures preceding the transition to the strong-localization mode, with an exponential decrease in the conductivity decreasing the temperature below 1 K [5]. Therefore, it is attributed to the manifestation of disorder at low temperatures due to defects, impurities, or dislocations. We note that the effect of disorder is in this case much stronger than in the weak localization mode. This work was initiated by the circumstance that the Aharonov–Bohm effect in this region has not been studied either theoretically or experimentally.

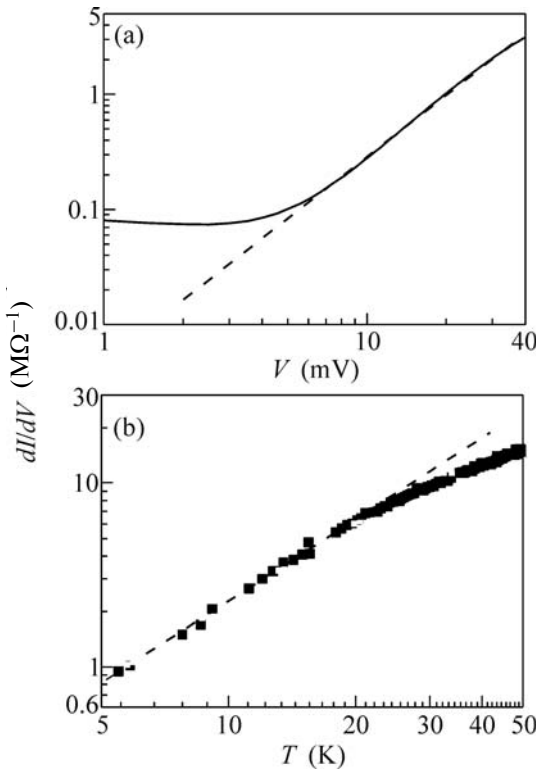


Fig. 1. Differential conductivity of MWNT sample no. 1 versus the (a) bias voltage at 1.5 K and (b) temperature at a current of 1 nA corresponding to the linear region of the current–voltage characteristic. The dashed curve is a power function with an exponent of 1.6.

The multiwall nanotubes under investigation were grown at Ecole Polytechnique, Palaiseau, France, by the CVD method in Al_2O_3 nanopores [15]. The outer diameter of the nanotubes $D \approx 20$ nm was determined by the pore diameter, and its length $L \approx 1 \mu\text{m}$, by the Al_2O_3 layer thickness. The nanotube orientation was determined by the nanopore orientation; i.e., they were normal to the Al_2O_3 layer surface. The measurements were performed on two samples chosen with respect to their resistance, which contained individual nanotubes with a low contact resistance [5]. The resistance of both samples at room temperature was about $10 \text{ k}\Omega$ and increased by more than two orders of magnitude during cooling to liquid-helium temperatures. The resistance was measured by the two-probe method. The current through the sample was set by a computer-controlled current source, while the voltage across the sample was measured by a nanovoltmeter. The magnetoresistance of the sample was measured in the Bitter magnet at Laboratoire National des Champs Magnétiques Intenses, Grenoble, France, in magnetic fields up to 32 T directed along the MWNT axis. The minimum attainable temperature was 1.2 K.

Figure 1 presents the differential conductivity $G(V) = dI/dV(V)$ of sample no. 1 as a function of (a)

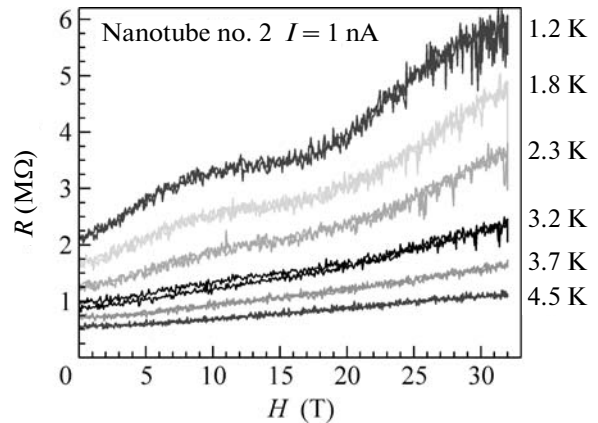


Fig. 2. Magnetoresistance $R(H)$ of nanotube no. 2 at different temperatures from (top) 1.2 to (bottom) 4.5 K in the magnetic field H directed along the nanotube axis. The measurement current was 1 nA and corresponded to the linear region of the current–voltage characteristic at all temperatures.

voltage at $T = 1.5$ K and (b) temperature under the conditions of linear current–voltage characteristics. It is seen that $G(V)$ is a constant up to a certain voltage $V = V_0 \approx 3$ mV, and then it increases with the voltage according to power law (1) with the exponent close to 1.6. Correspondingly, the low-temperature resistance of the samples measured at low currents (at $V < V_0$) increases with the temperature also by the power law with the same exponent of 1.6 (see Fig. 1b).

Figure 2 illustrates the magnetic-field dependences of magnetoresistance measured at different temperatures and a current of 1 nA corresponding to the voltage $V < V_0$ across the sample. At $T = 1.2$ K, magnetoresistance oscillations are clearly seen against the background of its monotonic increase. The oscillations were reproduced in the sweep $R(H)$ with increasing and decreasing magnetic field. They were also reproduced as the magnetic field direction was changed by 180° ($H \leftrightarrow -H$) (Fig. 3). It follows from Fig. 3 that the $R(H)$ dependence has an absolute maximum at $H = 0$. It is also seen that the oscillation amplitude decreases rapidly as the temperature increases, and the oscillations are almost unseen at $T > 3$ K.

The oscillation amplitude also decreases with increasing current (voltage) through the sample when the voltage across the sample is higher than V_0 . The oscillations almost disappear at currents larger than 10 nA (see Fig. 4).

Now we discuss the results. The subtraction of the monotonic background (Fig. 5) allows us to follow more than one and a half period of the magnetoresistance oscillatory part on both sides of $H = 0$. This analysis yields a period H_0 of about 18 T. The calculation with the use of this value and the flux quantum $\hbar c/e$ gives a nanotube diameter of 17.2 nm, which is close to the measured value 20 ± 3 nm. On the contrary, the

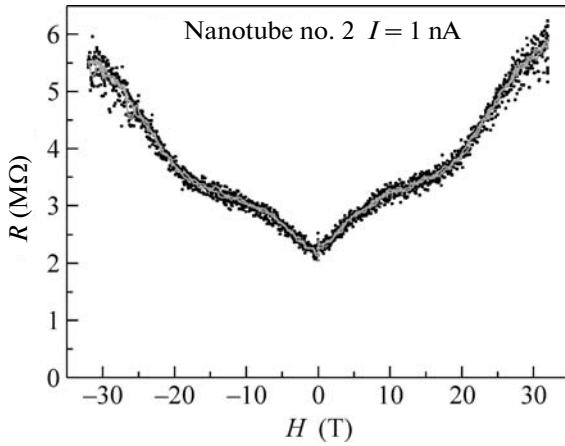


Fig. 3. Magnetoresistance $R(H)$ of nanotube no. 2 at $T = 1.2$ K for the parallel and antiparallel directions of the magnetic field.

calculation with the use of the flux half-quantum $\hbar c/2e$ gives an effective diameter of 12 nm, which differs considerably from the measured diameter. We note here that the MWNT shell makes a contribution to the Aharonov–Bohm oscillations [16, 17]. Therefore, the observed magnetoresistance oscillations correspond to the flux quantum per nanotube cross section. This conclusion is also confirmed by the positive monotonic magnetoresistance background and the absolute minimum of the $R(H)$ curve at $H \rightarrow \pm 0$. In the case of weak localization, which determines the magnetoresistance oscillation period in the flux as $\hbar c/2e$, the negative magnetoresistance background is

observed and the $R(H)$ curve has a maximum at $H \rightarrow \pm 0$.

The experimental result demonstrates a fairly non-trivial pattern. Under conditions close to strong localization, the period of observed Aharonov–Bohm oscillations in the flux is twice as large as that under weak localization conditions; i.e., it is the same as that in the ballistic mode. The Aharonov–Bohm effect under strong and near-strong localization conditions has not been theoretically analyzed. We may suppose qualitatively that under the transition to strong localization when the mean free path of the carriers remains longer than the nanotube perimeter, the carriers can undergo almost ballistic motion along the perimeter, and this determines the magnetoresistance period in the flux $\hbar c/e$. At the same time, the longitudinal motion with decreasing temperature exhibits the transition to one-dimensional localization, determining the increase in the resistance with decreasing temperature.

A similar phenomenological model of longitudinal transport on the defect-containing MWNTs was qualitatively considered in [14]. According to that model, the nanotube at low temperatures can be considered as a series chain of high-conductivity segments separated by the tunnel barriers formed by impurities, inclusions, etc. The increase in the nanotube resistance with decreasing temperature is determined by the barrier height and the possibility of the Coulomb blockade of the carriers, while the quasiballistic mode occurs inside the conducting segment. This model agrees qualitatively with our experiment. At low temperatures and low bias voltages, if the segment length and the mean free path of the carriers are longer than the nanotube perimeter, then the carriers in a mag-

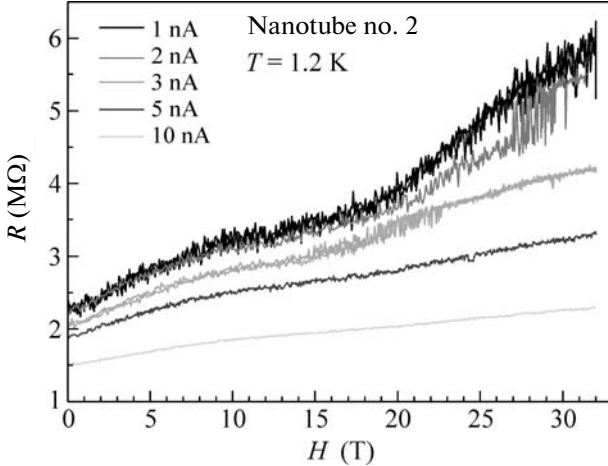


Fig. 4. Magnetoresistance $R(H)$ of nanotube no. 2 at $T = 1.2$ K and different measurement currents from (top) 1 to (bottom) 10 nA. The transition to a nonlinear mode occurred at a current of about 3 nA.

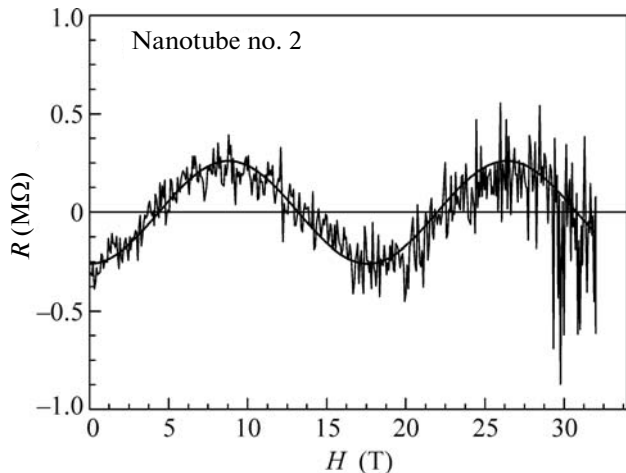


Fig. 5. Oscillatory part of the magnetoresistance of nanotube no. 2 after the subtraction of the monotonic part determined by the second-order fitting polynomial of H . The curve is the function $\Delta R = -A \cos(2\pi H/H_0)$ with two independent fitting parameters $A = 260$ kΩ and $H_0 = 17.6$ T.

netic field can undergo ballistic motion along the perimeter, which determines the oscillation period $\hbar c/e$ despite the high barrier-induced longitudinal resistance of the nanotube. As the temperature or the bias voltage increases, the carriers overcome the barriers more efficiently and simultaneously undergo efficient scattering. When the length of the carrier phase breaking becomes shorter than the nanotube perimeter, the Aharonov-Bohm oscillations are not observed.

We are grateful to G.E. Fedorov, M.V. Feigelman, A.S. Ioselevich, A.V. Shitov, S.N. Artemenko, and K.E. Nagaev for the discussions of our results, and to A.A. Sinchenko for technical assistance at the early stage of the experiments. The work was supported by the Russian Foundation for Basic Research (project nos. 08-02-01093a, 06-02-72551); L'Agence national de la recherche (French National Research Agency, grant no. ANR-07-BLAN-0136); the European Associated Laboratory organized by the Institute of Radio Engineering, Russian Academy of Sciences and Institut Néel; and the Russian Academy of Sciences (programs "Strongly Correlated Electrons in Solids and Structures" and "Physics of New Materials and Structures").

REFERENCES

1. S. Reich, C. Thomsen, and J. Maultzsch, *Carbon Nanotubes, Basic concepts and Physical Properties* (Wiley-VCN, Weinheim, 2004).
2. C. Dekker, Phys. Today **52**, 22 (1999).
3. J. Kong, E. Enilmes, T. W. Tombler, et al., Phys. Rev. Lett. **87**, 106801 (2001).
4. H. R. Shea, R. Martel, and Ph. Avouris, Phys. Rev. Lett. **84**, 4441 (2000).
5. J.-F. Dayen, X. Jehl, T. L. Wade, et al., Phys. Stat. Solidi B **243**, 3413 (2006).
6. B. Lassagne, J.-P. Clesiou, S. Nanot, et al., Phys. Rev. Lett. **98**, 176802 (2007).
7. G. Fedorov, A. Tselev, D. Jimenez, et al., Nano Lett. **7**, 960 (2007).
8. C. Schoenenberger, A. Bachtold, C. Strunk, et al., Appl. Phys. A **69**, 283 (1999).
9. D. Yu. Sharvin and Yu. V. Sharvin, Pis'ma Zh. Eksp. Teor. Fiz. **34**, 285 (1981) [JETP Lett. **34**, 272 (1981)].
10. B. L. Al'tshuler, A. G. Aronov, and B. Z. Spivak, Pis'ma Zh. Eksp. Teor. Fiz. **33**, 101 (1981) [JETP Lett. **33**, 94 (1981)].
11. J.-F. Dayen, T. L. Wade, M. Konczykowski, et al., Phys. Rev. B **72**, 073402 (2005).
12. R. Eger, Phys. Rev. Lett. **83**, 5547 (1999).
13. M. V. Feigelman and A. S. Ioselevich, Pis'ma Zh. Eksp. Teor. Fiz. **88**, 882 (2008) [JETP Lett. **88**, 767 (2008)].
14. J.-F. Dyen, T.L. Wade, and G. Rizza, Eur. Phys. J.: Appl. Phys. **48**, 10604 (2009).
15. T. L. Wade and J. E. Wegrow, Eur. Phys J.: Appl. Phys. **29**, 3 (2005).
16. A. Bachtold, C. Strunk, J.-P. Salvetat, et al., Nature **397**, 673 (1999).
17. S. Frank, P. Poncharal, Z. L. Wang, et al., Science **280**, 1744 (2001).

Translated by E. Perova